



Article

Verrucosidin Derivatives from the Deep Sea Cold-Seep-Derived Fungus *Penicillium polonicum* CS-252

Yanhe Li ^{1,2,3}, Xiaoming Li ^{1,2}, Xin Li ^{1,2} , Suiqun Yang ^{1,2}, Bingui Wang ^{1,2,3,4,*} and Honglei Li ^{1,2,*}

- ¹ CAS and Shandong Province Key Laboratory of Experimental Marine Biology, Institute of Oceanology, Chinese Academy of Sciences, Nanhai Road 7, Qingdao 266071, China; liyanhe1025@163.com (Y.L.); lixmqdio@126.com (X.L.); lixin871014@163.com (X.L.); suiqunyang@163.com (S.Y.)
- ² Laboratory of Marine Biology and Biotechnology, Qingdao National Laboratory for Marine Science and Technology, Wenhai Road 1, Qingdao 266237, China
- ³ College of Marine Science, University of Chinese Academy of Sciences, Yuquan Road 19A, Beijing 100049, China
- ⁴ Center for Ocean Mega-Science, Chinese Academy of Sciences, Nanhai Road 7, Qingdao 266071, China
- * Correspondence: wangbg@ms.qdio.ac.cn (B.W.); lihonglei@qdio.ac.cn (H.L.);
Tel.: +86-532-82898553 (B.W.); +86-532-82898890 (H.L.)

Abstract: Six novel verrucosidin derivatives, namely, poloncosidins A–F (1–6), together with one known analogue (7), were isolated and identified from the deep-sea-derived fungus *Penicillium polonicum* CS-252, which was obtained from cold-seep sediments collected in the South China Sea at a depth of 1183 m. Their structures were mainly established on the basis of a detailed interpretation of NMR spectroscopic and mass spectrometric data. The relative and absolute configurations of compounds 1–6 were determined by ECD calculations and a DP4+ probability analysis. Compounds 1–5 represent the first examples of verrucosidins with a 2,5-dihydrofuran ring which is uncommon among the known analogues. These compounds exhibited inhibitory activities against several human and aquatic pathogens with MIC values ranging from 4 to 32 µg/mL.

Keywords: deep-sea-derived fungus; *Penicillium polonicum*; verrucosidin derivatives; structure elucidation; antimicrobial activity



Citation: Li, Y.; Li, X.; Li, X.; Yang, S.; Wang, B.; Li, H. Verrucosidin Derivatives from the Deep Sea Cold-Seep-Derived Fungus *Penicillium polonicum* CS-252. *Int. J. Mol. Sci.* **2022**, *23*, 5567. <https://doi.org/10.3390/ijms23105567>

Academic Editors: Maria Costantini, Valerio Zupo and Nadia Ruocco

Received: 9 April 2022

Accepted: 5 May 2022

Published: 16 May 2022

Publisher's Note: MDPI stays neutral with regard to jurisdictional claims in published maps and institutional affiliations.



Copyright: © 2022 by the authors. Licensee MDPI, Basel, Switzerland. This article is an open access article distributed under the terms and conditions of the Creative Commons Attribution (CC BY) license (<https://creativecommons.org/licenses/by/4.0/>).

1. Introduction

Verrucosidins belong to a family of highly reduced polyketides, generally sharing a methylated α -pyrone, a conjugated polyene linker, and an epoxidated tetrahydrofuran ring [1]. All verrucosidin derivatives previously isolated and characterized from the fungal genus *Penicillium* were found to possess bioactivities such as antibacterial and GRP78/BiP down-regulator activities [2,3]. *Penicillium polonicum* is a ubiquitous fungus found as saprophyte in diverse environments [4], from which bioactive molecules with diverse chemical structures have been reported including diketopiperazine, α -pyrone derivative, dimeric anthraquinone, and taxol [5–10]. The verrucosidin biosynthesis gene cluster was also reported in *P. polonicum*, which confirmed the ability of the fungus to produce related secondary metabolites [11,12].

In our ongoing research for the discovery of bioactive secondary metabolites from marine-derived fungi [13–15], the fungal strain *P. polonicum* CS-252, which was obtained from sediments collected at the deep-sea cold seep area in the South China Sea, attracted our attention due to its unique HPLC profiles which showed peaks with different UV absorptions from those in our HPLC database. A chemical investigation of the culture extract of *P. polonicum* CS-252 led to the characterizations of six new verrucosidin derivatives, designated as poloncosidins A–F (1–6, Figure 1), together with a known analogue, deoxyverrucosidin (7). Among them, compounds 1–5 represent the first examples of verrucosidins with a 2,5-dihydrofuran ring. Details of the isolation, purification, structure elucidation, and biological evaluation of compounds 1–7 are provided herein.

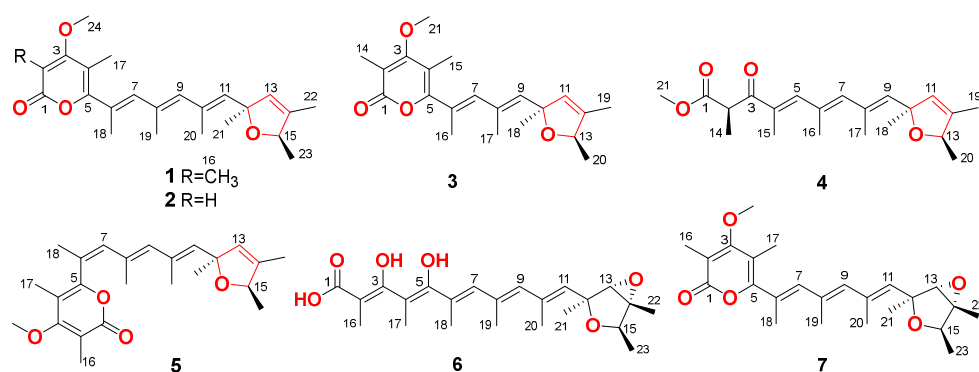


Figure 1. Chemical structures of compounds 1–7.

2. Results and Discussion

The fungus *P. polonicum* CS-252 was cultured on a rice solid medium for chemical investigation. The obtained culture was extracted thoroughly with EtOAc to produce an organic extract that was further fractionated and purified with a combination of column chromatography over Lobar LiChroprep RP-18, Si gel, and Sephadex LH-20 as well as by prep. TLC to yield compounds 1–7.

Poloncosidin A (1) was obtained as a colorless oil and its molecular formula was assigned as $C_{24}H_{32}O_4$ on the basis of HRESIMS data, corresponding to nine indices of hydrogen deficiency. The 1H -NMR and HSQC spectra of 1 (Table 1 and Figure S5) revealed the signals of nine methyls with one doublet (δ_H 1.16, $J = 6.4$ Hz) eight singlets (δ_H 1.33, 1.66, 1.88, 1.93, 1.95, 1.96, 2.00, and 3.82), four singlet olefinic protons (δ_H 5.53, 5.61, 5.93, and 6.16), and a quartet proton at δ_H 4.62 (1H, q, $J = 6.4$ Hz). The ^{13}C -NMR and DEPT data (Table 2 and Figure S3) indicated all 24 carbon resonances including nine methyls, five methines (with four olefinic at δ_C 127.2, 137.1, 137.2, and 139.1 as well as an oxygenated at δ_C 81.6), and ten nonprotonated carbons (with eight olefinic, one carbonyl, and one oxygenated). The aforementioned spectroscopic data suggested the characteristics of a verrucosidin derivative, which are similar to those of deoxyverrucosidin (7) previously described in *Penicillium* sp. in 2005, with the difference that the epoxide moiety in 7 was replaced by a double bond in 1. This difference was supported by the NMR evidence that signals for an oxygenated methine (δ_H 3.45; δ_C 67.5, CH-13) and an oxygenated nonprotonated carbon (δ_C 67.4, C-14) in the NMR spectra of deoxyverrucosidin (7) [3] were not present in those of 1, while resonances for an olefinic methine (δ_H 5.61, H-13; δ_C 127.2, C-13) and an olefinic nonprotonated carbon (δ_C 138.2, C-14) were observed in the NMR spectra of 1 (Tables 1 and 2). These data indicated that the epoxidated tetrahydrofuran ring in deoxyverrucosidin was replaced by a 2,5-dihydrofuran ring in 1. This deduction was supported by the key HMBC from H-11 (δ_H 5.53) and H₃-21 (δ_H 1.33) to C-13 (δ_C 127.2) and from H₃-22 (δ_H 1.66) to C-13, C-14 (δ_C 138.2), and C-15 (δ_C 81.6) (Figure 2). The planar structure of 1 was thus identified as the first example of verrucosidins possessing a 2,5-dihydrofuran moiety.

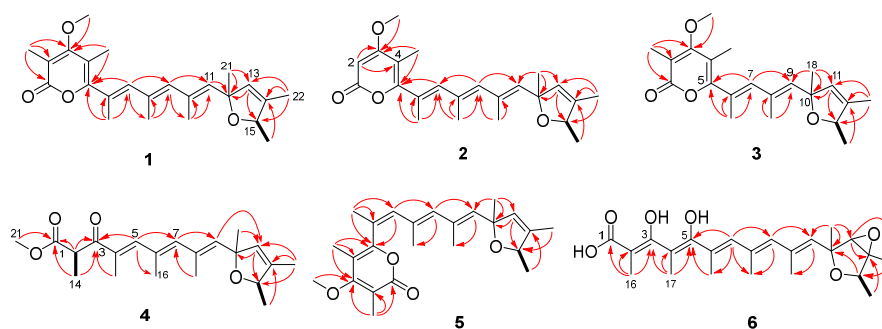


Figure 2. COSY (black bold lines) and key HMBC (red arrows) cross-peaks of compounds 1–6.

Table 1. $^1\text{H-NMR}$ Data of Compounds 1–6 (500 MHz, $\text{DMSO-}d_6$, δ in ppm, J in Hz).

No	1	2	3	4	5	6
2		5.61, s		4.52, q (7.0)		
5				7.19, s		
7	6.16, s	6.13, s	6.08, s	6.14, s	6.26, s	5.92, s
9	5.93, s	5.93, s	5.63, s	5.60, s	5.84, s	5.83, s
11	5.53, s	5.53, s	5.62, s	5.61, s	5.39, s	5.54, s
13	5.61, s	5.61, s	4.63, q (6.4)	4.63, q (6.4)	5.56, s	3.63, s
14			1.92, s	1.21, d (7.0)		
15	4.62, q (6.4)	4.61, q (6.4)	1.94, s	1.89, s	4.59, q (6.5)	4.00, q (6.7)
16	1.93, s		1.95, s	2.00, s	1.94, s	1.57, s
17	1.96, s	1.89, s	1.92, s	1.90, s	1.76, s	1.72, s
18	2.00, s	2.00, s	1.33, s	1.33, s	1.94, s	1.93, s
19	1.95, s	1.95, s	1.67, s	1.66, s	1.58, s	1.94, s
20	1.88, s	1.87, s	1.17, d (6.4)	1.16, d (6.4)	1.79, s	1.92, s
21	1.33, s	1.32, s	3.81, s	3.60, s	1.28, s	1.28, s
22	1.66, s	1.66, s			1.63, s	1.39, s
23	1.16, d (6.4)	1.16, d (6.4)			1.12, d (6.5)	1.11, d (6.7)
24	3.82, s	3.84, s			3.80, s	

Table 2. $^{13}\text{C-NMR}$ Data of Compounds 1–6 (125 MHz, $\text{DMSO-}d_6$, δ in ppm).

No	1	2	3	4	5	6
1	164.0, C	162.5, C	164.0, C	171.4, C	164.4, C	165.3, C
2	108.6, C	87.9, CH	108.8, C	45.6, CH	108.8, C	89.9, C
3	168.0, C	170.7, C	168.0, C	198.5, C	168.5, C	177.0, C
4	108.9, C	106.0, C	108.8, C	132.9, C	109.5, C	111.3, C
5	158.6, C	160.6, C	158.4, C	145.5, CH	155.9, C	155.4, C
6	126.3, C	126.3, C	126.3, C	131.8, C	125.6, C	132.3, C
7	139.1, CH	139.1, CH	138.9, CH	140.8, CH	133.0, CH	135.2, CH
8	131.3, C	131.2, C	130.1, C	130.6, C	131.3, C	129.7, C
9	137.1, CH	137.1, CH	138.3, CH	138.3, CH	137.3, CH	134.6, CH
10	130.7, C	130.7, C	87.3, C	87.3, C	130.6, C	134.4, C
11	137.2, CH	137.2, CH	127.1, CH	127.1, CH	137.7, CH	132.8, CH
12	87.3, C	87.3, C	138.4, C	138.4, C	87.3, C	79.4, C
13	127.2, CH	127.3, CH	81.6, CH	81.6, CH	127.2, CH	66.4, CH
14	138.2, C	138.3, C	9.9, CH_3	14.3, CH_3	138.3, C	66.9, C
15	81.6, CH	81.6, CH	11.6, CH_3	13.0, CH_3	81.6, CH	75.9, CH
16	9.9, CH_3		15.9, CH_3	17.8, CH_3	10.0, CH_3	9.9, CH_3
17	11.7, CH_3	10.8, CH_3	17.4, CH_3	17.6, CH_3	10.5, CH_3	12.3, CH_3
18	16.2, CH_3	16.2, CH_3	27.6, CH_3	27.6, CH_3	22.7, CH_3	16.7, CH_3
19	17.9, CH_3	17.9, CH_3	11.8, CH_3	11.8, CH_3	15.7, CH_3	18.4, CH_3
20	17.8, CH_3	17.9, CH_3	20.5, CH_3	20.5, CH_3	17.7, CH_3	18.3, CH_3
21	27.6, CH_3	27.7, CH_3	60.2, CH_3	51.9, CH_3	27.6, CH_3	21.9, CH_3
22	11.6, CH_3	11.8, CH_3			11.8, CH_3	13.4, CH_3
23	20.5, CH_3	20.5, CH_3			20.5, CH_3	18.6, CH_3
24	60.2, CH_3	56.7, CH_3			60.3, CH_3	

The relative configuration of compound **1** was established by an analysis of its NOESY data (Figure 3). Key NOESY enhancement from H-15 to H₃-21 indicated the cofacial orientation of these protons, which established the relative configuration of the 2,5-dihydrofuran moiety. The geometries of the double bonds at C-6, C-8, and C-10 were determined to be *E* configurations by the NOESY correlations from H-7 to H-9 and H₃-17 and from H-9 to H-11 (Figure 3). To establish the absolute configuration of **1**, the time-dependent density functional (TDDFT)-ECD calculations at the BH&HLYP/TZVP level were performed in Gaussian 09. The calculated ECD spectrum for the (12*S*,15*R*)-isomer of compound **1** matched well with the experimental curve, leading to the establishment of the absolute configuration of **1** as 12*S*, 15*R* (Figure 4).

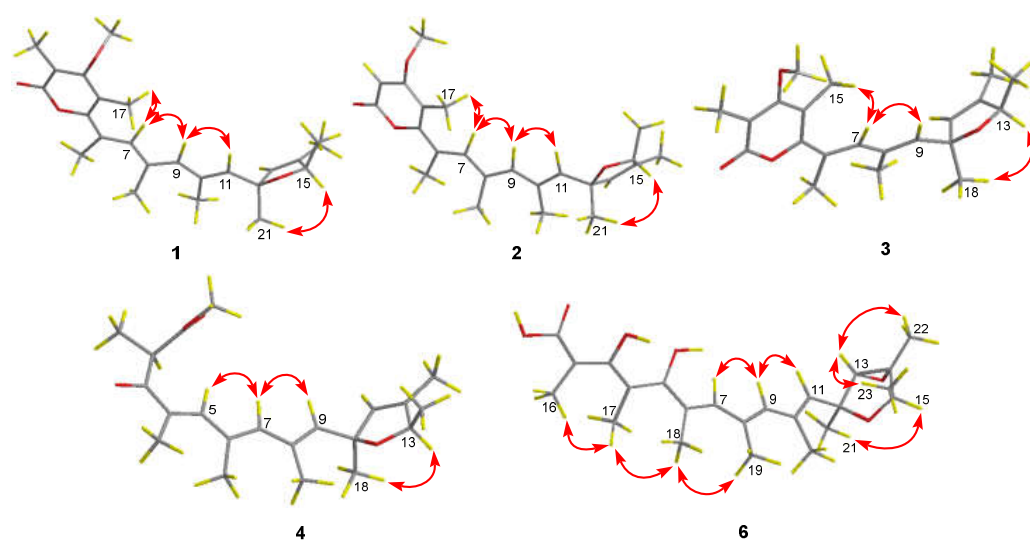


Figure 3. Key NOESY correlations of compounds 1–4 and 6.

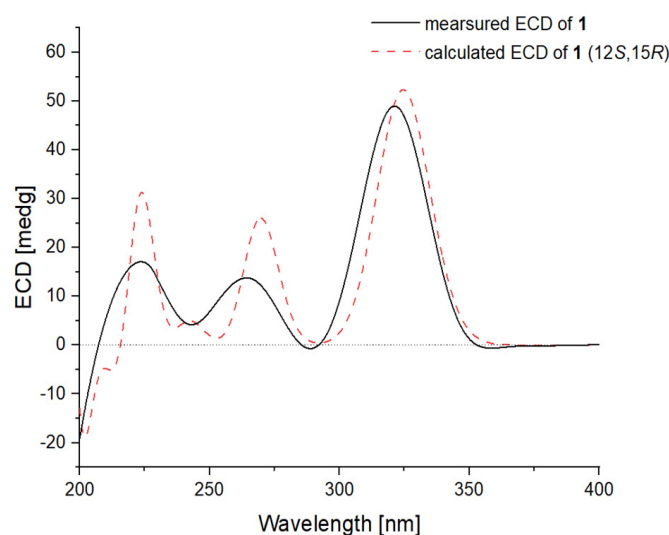


Figure 4. Experimental ECD spectrum of **1** (black line) compared with that calculated for (12*S*,15*R*)-isomer of **1** at BH&HLYP/TZVP level (red dashed line).

Poloncosidin B (**2**) was obtained as a colorless oil and the molecular formula was assigned as $C_{23}H_{30}O_4$ based on an analysis of the HRESIMS data with the same hydrogen deficiency index as that of **1**. A comprehensive analysis of the 1H - and ^{13}C -NMR data of **2** indicated a similar structure to that of **1**, only differing in the absence of a substituent. Signals for a methyl (δ_H 1.93; δ_C 9.9, CH_3 -16) and an olefinic nonprotonated carbon (δ_C 108.6, C-2) in the NMR spectra of **1** were found to be absent in those of **2** (Tables 1 and 2). In contrast, compound **2** exhibited an additional resonance at δ_H 5.61 (1H, s, H-2) in the 1H -NMR spectrum that correlates with an olefinic methine carbon at δ_C 87.9 (C-2), accounting for the shielding effect of the carbonyl group at C-1. The key HMBC correlations from H-2 to C-3 (δ_C 170.7) and C-4 (δ_C 106.0) as well as other key HMBC and COSY correlations (Figure 2) established the structure of compound **2** as shown.

The relative configuration of the 2,5-dihydrofuran ring and the geometries of the double bonds at C-6, C-8, and C-10 were determined to be the same as those of compound **1** with an analysis of the NOESY correlations (Figure 3). The absolute configuration of **2** was assigned as 12*S* and 15*R*, which was evidenced by a comparison of the overlaid experimental and calculated ECD curves at the BH&HLYP/TZVP level (Figure 5).

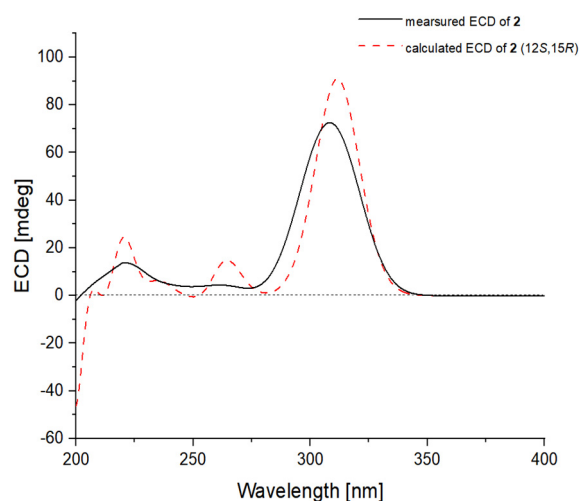


Figure 5. Experimental ECD spectrum of **2** (black line) comparing with that calculated for (12*S*,15*R*)-isomer of **2** at BH&HLYP/TZVP level (red dashed line).

The molecular formula of poloncosidin C (**3**) was determined as $C_{21}H_{28}O_4$ according to the HRESIMS ion peaks at m/z 345.2057 $[M + H]^+$ (calcd for $C_{21}H_{29}O_4$, 345.2060) and 367.1875 $[M + Na]^+$ (calcd for $C_{21}H_{28}O_4Na$, 367.1880), required eight indices of hydrogen deficiency. Detailed interpretation of the 1H - and ^{13}C -NMR data revealed **3** to be structurally related to compounds **1** and **2**, featuring a methylated α -pyrone moiety and a 2,5-dihydrofuran ring linked with a shorter polyene linker. This deduction was supported by the NMR evidence that resonances for one of the trisubstituted double bonds in the conjugated polyene linker, comprising a singlet methyl (δ_H 1.95; δ_C 17.9, CH_3 -19), a singlet olefinic methine (δ_H 5.93; δ_C 137.1, CH -9), and an olefinic nonprotonated carbon (δ_C 131.3, C -8) in the NMR spectra of **1** disappeared in those of **3**. Combined with the key HMBC correlations from H-7 (δ_H 6.08) to C-5 (δ_C 158.4) and C-9 (δ_C 138.3) as well as from H₃-18 (δ_H 1.33) to C-9 (δ_C 138.3), C-10 (δ_C 87.3) and C-11 (δ_C 127.1) (Figure 2), the planar structure of compound **3** was thus established.

The observed NOESY correlations between H-13 and H₃-18 helped to establish the relative configuration of the 2,5-dihydrofuran moiety (Figure 3). The *E*-geometry of the double bonds at C-6 and C-8 was determined by the observed NOEs from H-7 to H-9 and H₃-15 (Figure 3). The absolute configuration of **3** was assigned as 10*S* and 13*R* based on the results of the TDDFT-ECD calculations at the BH&HLYP/TZVP level as shown in Figure 6.

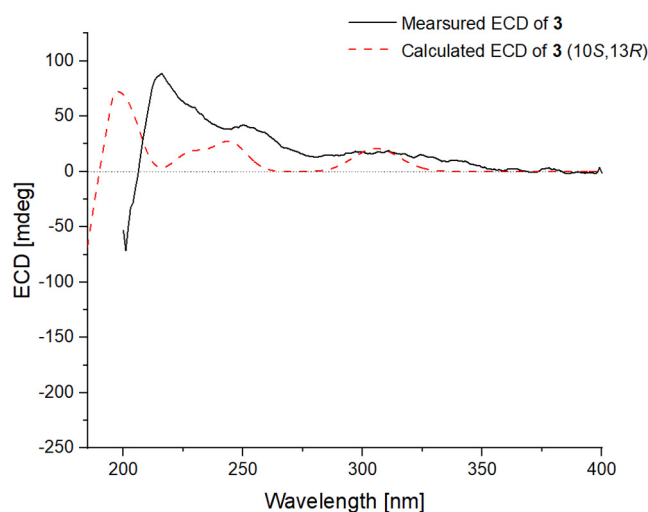


Figure 6. Experimental ECD spectrum of **3** (black line) comparing with that calculated for (10*S*,13*R*)-isomer of **3** at BH&HLYP/TZVP level (red dashed line).

Poloncosidin D (**4**) was isolated as a colorless oil. The molecular formula was established as $C_{21}H_{30}O_4$ from its HRESIMS data with seven indices of hydrogen deficiency. The 1H - and ^{13}C -NMR spectra of **4** revealed a 2,5-dihydrofuran moiety with three sets of conjugated double bonds, conforming to the characteristics of verrucosidin derivatives. However, additional resonances for two carbonyl carbons (δ_C 198.5, C-3 and 171.4, C-1) were observed in the ^{13}C -NMR spectrum of **4** that are quite different from those of compounds **1–3**. The COSY correlation from H-2 (δ_H 4.52) to H₃-14 (δ_H 1.21) as well as HMBC correlations from H₃-14 to C-1 and C-3, from H-5 (δ_H 7.19) to C-3, C-7 (δ_C 140.8), and C-16 (δ_C 17.8), and from H₃-21 (δ_H 3.60) to C-1 established the structure of **4**, which possesses the same polyketide skeleton as that of compound **3**, but without the formation of the α -pyrone moiety.

The relative configuration of **4** was established by the observed NOESY correlations (Figure 3), except for the stereogenic center of C-2. To establish the stereochemistry, TDDFT-ECD calculations for four possible isomers of **4** [**4a**-(2*R*,10*S*,13*R*), **4b**-(2*S*,10*S*,13*R*), **4c**-(2*R*,10*R*,13*S*), and **4d**-(2*S*,10*R*,13*S*)] (Figure 7) were performed, and then two isomers [**4a**-(2*R*,10*S*,13*R*) and **4b**-(2*S*,10*S*,13*R*)] were recommended for **4** (Figure 8), which were further clarified by the DP4+ probability analysis. Both the proton and carbon data of the two possible isomers were calculated based on the DP4+ protocol and the results were analyzed with the experimental values [16]. The statistical analysis indicated that the isomer [**4a**-(2*R*,10*S*,13*R*)] was the equivalent structure with a probability of 99.91% (Figures 8 and S42). The absolute configuration of **4** was thus assigned.

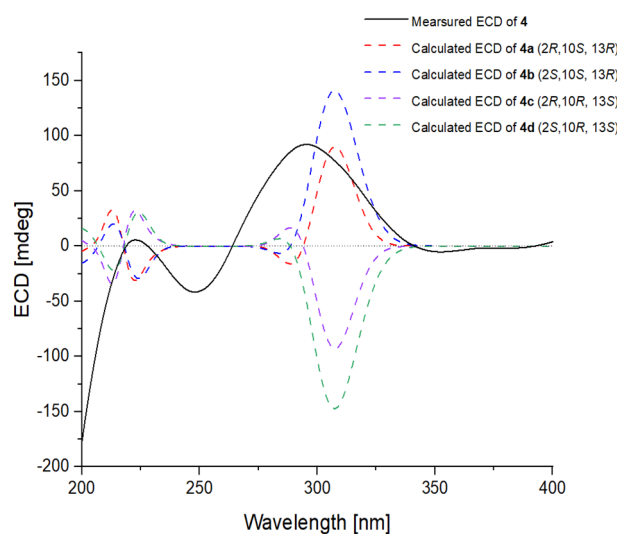


Figure 7. Experimental ECD spectrum of **4** (black line) compared with those calculated for **4a**-(2*R*,10*S*,13*R*), **4b**-(2*S*,10*S*,13*R*), **4c**-(2*R*,10*R*,13*S*), and **4d**-(2*S*,10*R*,13*S*) of **4** at BH&HLYP/TZVP level (red, blue, purple and green dashed lines, respectively).

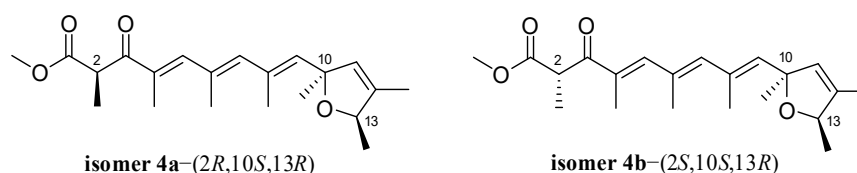


Figure 8. Two possible isomers of compound **4** for DP4+ probability analysis.

The molecular formula of poloncosidin E (**5**) was assigned as $C_{24}H_{32}O_4$ based on the accurate mass data measured by HRESIMS, which was identical to that of **1**. The 1H - and ^{13}C -NMR data of **5** were virtually identical to those obtained for **1** (Tables 1 and 2), except for the shielded location of C-5 at δ_C 155.9 and de-shielded location of C-18 at δ_C 22.7 in the ^{13}C -NMR spectrum of **5**, conforming to the γ -gauche effect [17]. Moreover, resonances for

C-6 (δ_C 125.6) and C-7 (δ_C 133.0) also moved to the shielded field in the ^{13}C -NMR spectrum of **5**. A detailed analysis of the COSY and HMBC correlations of **5** (Figure 2) revealed that it possessed the same planar structure as **1**, but with *Z*-geometry for the double bond at C-6. The structure of compound **5** was thus established with the above NMR data.

Unfortunately, the NOESY spectrum of **5** was not obtained due to instability and low abundance, and compound **5** was actually isolated as a highly impure mixture. To further define the geometry of the double bond at C-6, a DP4+ probability analysis was performed. The steric configuration of the 2,5-dihydrofuran moiety was determined as the same as that of compounds **1**–**4** based on the NMR data comparisons and biosynthetic origins. Two possible isomers [**5a**-(6*E*,12*S*,15*R*) and **5b**-(6*Z*,12*S*,15*R*)] of compound **5** were thus generated for DP4+ calculations (Figure 9). The ^{13}C -NMR data calculated for the isomer [**5b**-(6*Z*,12*S*,15*R*)] matched well with the experimental data of **5** (probability = 100%), which led to the assignment of the steric configuration for **5**.

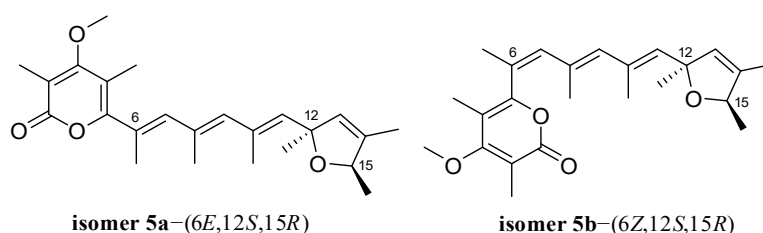


Figure 9. Two possible isomers of compound **5** for DP4+ probability analysis.

Poloncosidin F (**6**) was obtained as a colorless oil with a molecular formula of $\text{C}_{23}\text{H}_{32}\text{O}_6$ as determined by the HRESIMS data. Its ^1H - and ^{13}C -NMR data (Tables 1 and 2) revealed a close structural relationship with deoxyverrucosidin (**7**) [3]. One of the visible differences were that the signals for a methoxy group 3- OCH_3 (δ_{H} 3.83; δ_{C} 60.2) in the NMR spectra of deoxyverrucosidin (**7**) were absent in those of **6**. Moreover, a de-shielded resonance for C-3 (δ_{C} 177.0) and a shielded field shift for C-2 (δ_{C} 89.9) were clearly observed in the ^{13}C -NMR spectrum of **6** (Table 2), compared to those of **7** [3]. These spectroscopic features as well as in considering the molecular formula revealed that the ester linkage of the α -pyrone ring in deoxyverrucosidin (**7**) was hydrolyzed in **6**. Supported by the HMBC correlations from H_3 -16 (δ_{H} 1.57) to C-1 (δ_{C} 165.3), C-2, and C-3 as well as from H_3 -17 (δ_{C} 1.72) to C-3, C-4 (δ_{C} 111.3), and C-5 (δ_{C} 155.4) (Figure 2), the planar structure of **6** was established.

The *E*-geometry of five conjugated double bonds at C-2, C-4, C-6, C-8, and C-10 were assigned by the NOE correlations from H_3 -17 to H_3 -16 and H_3 -18, from H_3 -18 to H_3 -19, and from H-9 to H-7 and H-11. NOE correlations from H-13 to H_3 -22 and H_3 -23 indicated the cofacial orientation of these groups, while the cross-peak from H-15 to H_3 -21 assigned these groups at the opposite face. Similarly, the absolute configuration of **6** was determined by the TDDFT-ECD calculations in Gaussian 09. The ECD spectrum calculated at the BH&HLYP/TZVP level for isomer (12*S*,13*S*,14*R*,15*R*)-**6** matched well with the experimental curve (Figure 10), leading to the establishment of the absolute configuration of **6**.

In addition to the new compounds **1**–**6**, the known analogue deoxyverrucosidin (**7**) was also isolated and identified by a detailed spectroscopic analysis and comparisons with the reported data [3].

The obtained compounds, except for compound **5**, were assayed for antimicrobial activities against human-, aqua-, and plant-pathogenic microbes. These compounds showed inhibitory activity against some of the tested bacterial strains ($\text{MIC} \leq 32 \mu\text{g/mL}$, Table 3). Among them, compounds **4** and **6** displayed inhibitory activity against *Escherichia coli* EMBLC-1, *Klebsiella pneumoniae* EMBLC-3, *Pseudomonas aeruginosa* QDIO-4, *Vibrio alginolyticus* QDIO-5, and *V. parahemolyticus* QDIO-8 with MIC values ranging from 4 to $32 \mu\text{g/mL}$. Compound **4** also inhibited methicillin-resistant *Staphylococcus aureus* (MRSA) EMBLC-4 with an MIC value of $16 \mu\text{g/mL}$. Moreover, compound **1** showed activity against *P. aeruginosa* QDIO-4, *V. alginolyticus* QDIO-5, and *V. parahemolyticus* QDIO-8 with MICs 8.0, 8.0, and

4.0 $\mu\text{g/mL}$, respectively, whereas compound 7 was bactericidal against *P. aeruginosa* QDIO-4 and *V. parahemolyticus* QDIO-8 (each with an MIC value of 8.0 $\mu\text{g/mL}$). These data indicated that verrucosidin derivatives without the formation of the α -pyrone moiety exhibited a broad spectrum of antimicrobial activity against the tested strains (4 and 6 vs. 1–3, and 7). In addition, the methylation at C-2 and the 2,5-dihydrofuran ring in these compounds enhanced their activities (1 vs. 2 and 7), while the absence of a trisubstituted double bond in the polyene linker (compound 3) likely had an adverse effect on the antibacterial activity.

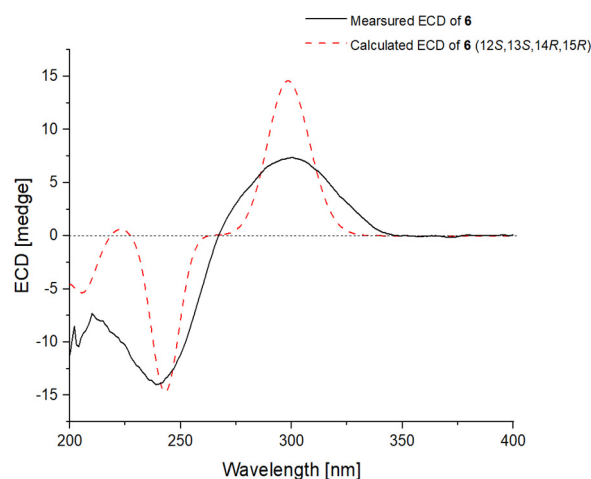


Figure 10. Experimental ECD spectrum of 6 (black line) compared with that calculated for (12S,13S,14R,15R)-isomer of 6 at BH&HLYP/TZVP level (red dashed line).

Table 3. Antimicrobial Activities of Compounds 1–4, 6, and 7 (MIC, $\mu\text{g/mL}$).

Strains	Compounds						Chloramphenicol ^b
	1	2	3	4	6	7	
<i>E. coli</i>	16	– ^a	–	4.0	32	32	1.0
<i>K. pneumoniae</i>	–	32	–	32	16	–	4
MRSA	–	–	–	16	–	–	4
<i>P. aeruginosa</i>	8.0	16	8.0	16	16	8.0	1.0
<i>V. alginolyticus</i>	8.0	–	16	8.0	8.0	32	0.5
<i>V. parahemolyticus</i>	4.0	8.0	–	16	16	8.0	1.0

^a (–) = MIC > 32 $\mu\text{g/mL}$. ^b Chloramphenicol as positive control.

3. Experimental Section

3.1. General Experimental Procedures

The instruments, organic solvents, and reagents used in this work were the same as those used in our previous reports [13–15].

3.2. Fungal Material

The fungus *P. polonicum* CS-252 was isolated from the cold seep sediments, which were collected from South China Sea (depth 1183 m) in September 2020. The fungal strain was identified as *Penicillium polonicum* based on the ITS region sequence, which is the same (100%) as that of *P. polonicum* FNG3 (with accession no. MZ301257.1). The sequence data were deposited in GenBank with the accession no. OK175489.1. The strain is being preserved at the Key Laboratory of Experimental Marine Biology, Institute of Oceanology, Chinese Academy of Sciences (IOCAS).

3.3. Fermentation, Extraction and Isolation

For chemical investigations, 1 L Erlenmeyer flasks with a solid medium containing rice were autoclaved at 120 °C for 20 min before inoculation. Each flask contained 70 g rice, 0.3 g peptone, 0.5 g yeast extract, 0.2 g corn steep liquor, 0.1 g monosodium glutamate,

and 100 mL of naturally sourced and filtered seawater obtained from the Huiquan Gulf of the Yellow Sea near the campus of IOCAS. The fresh mycelia of *P. polonicum* CS-252 were grown on a PDA medium at 28 °C for seven days, inoculated into the autoclaved medium and then statically cultured for 30 days at room temperature. The fermented rice substrate was fragmented mechanically and extracted thoroughly with EtOAc. The above EtOAc solutions were combined and concentrated under reduced pressure to produce 70.0 g organic extract.

The extract was subjected to vacuum liquid chromatography (VLC) over Si gel and fractionated using solvent mixtures of increasing polarity consisting of petroleum ether (PE) and EtOAc (20:1 to 1:1) and finally with CH₂Cl₂-MeOH (50:1 to 1:1) to yield 10 fractions (Frs. 1–10). Purification of Fr. 3 (4.1 g), performed with column chromatography (CC) over Lobar LiChroprep RP-18 with a MeOH-H₂O gradient (from 1:9 to 10:0), yielded 10 subfractions (Frs. 3.1–3.10). Fr. 3.7 (113 mg) was purified with CC on Sephadex LH-20 (MeOH) to obtain compounds **4** (7.8 mg) and **6** (3.8 mg). Fr. 3.8 (215.0 mg) was subjected to CC on Si gel (CH₂Cl₂-MeOH, 200:1 to 150:1), and then purified by prep. TLC and CC on Sephadex LH-20 (MeOH) provided compounds **1** (52.4 mg), **2** (6.2 mg), and **3** (4.0 mg). Fr. 3.9 (75 mg) was purified with CC on Si gel (CH₂Cl₂-MeOH, 300:1), and then purified with CC on Sephadex LH-20 (MeOH) to obtain compound **7** (23.1 mg). Fr. 4 (10.4 g) was further fractionated with CC over Lobar LiChroprep RP-18 elution with a MeOH-H₂O gradient (from 1:9 to 10:0) to yield 10 subfractions (Frs. 4.1–4.10). Fr. 4.3 (87 mg) was separated with CC on Si gel and Sephadex LH-20 (MeOH) to obtain compound **5** (7.4 mg).

Poloncosidin A (**1**) colorless oil; $[\alpha]_D^{25} = +65$, c 0.10, MeOH; UV (MeOH) λ_{\max} (log ϵ) 229 (2.64), 303 (2.23) nm; ECD (1.04 mM, MeOH) λ_{\max} ($\Delta\epsilon$) 200 (−1.39), 223 (+1.39), 265 (+1.01), 321 (+3.56) nm; ¹H- and ¹³C-NMR data, Tables 1 and 2; HRESIMS m/z 385.2373 [M + H]⁺ (calcd for C₂₄H₃₃O₄, 385.2373).

Poloncosidin B (**2**) colorless oil; $[\alpha]_D^{25} = +51$, c 0.10, MeOH; UV (MeOH) λ_{\max} (log ϵ) 230 (2.66), 304 (2.25) nm; ECD (1.10 mM, MeOH) λ_{\max} ($\Delta\epsilon$) 221 (+1.03) nm, 261 (+0.32) nm, 308 (+5.77) nm; ¹H- and ¹³C-NMR data, Tables 1 and 2; HRESIMS m/z 371.2216 [M + H]⁺ (calcd for C₂₄H₃₁O₄, 371.2217).

Poloncosidin C (**3**) colorless oil; $[\alpha]_D^{25} = +33$, c 0.15, MeOH; UV (MeOH) λ_{\max} (log ϵ) 246 (2.68), 315 (3.03) nm; ECD (1.16 mM, MeOH) λ_{\max} ($\Delta\epsilon$) 201 (−1.86), 217 (+2.24), 250 (+1.09), 311 (+0.49) nm; ¹H- and ¹³C-NMR data, Tables 1 and 2; HRESIMS m/z 345.2057 [M + H]⁺ (calcd for C₂₁H₂₉O₄, 345.2060), 367.1875 [M + Na]⁺ (calcd for C₂₁H₂₈O₄Na, 367.1880).

Poloncosidin D (**4**) colorless oil; $[\alpha]_D^{25} = +38$, c 0.14, MeOH; UV (MeOH) λ_{\max} (log ϵ) 232 (2.63) nm, 299 (2.32) nm; ECD (1.16 mM, MeOH) λ_{\max} ($\Delta\epsilon$) 200 (−2.93), 223 (+0.05), 251 (−0.72), 296 (+1.64) nm; ¹H- and ¹³C-NMR data, Tables 1 and 2; HRESIMS m/z 369.2031 [M + Na]⁺ (calcd for C₂₁H₃₀O₄Na, 369.2036).

Poloncosidin E (**5**) colorless oil; ¹H- and ¹³C-NMR data, Tables 1 and 2; HRESIMS m/z 385.2372 [M + H]⁺ (calcd for C₂₄H₃₃O₄, 385.2373), 407.2190 [M + Na]⁺ (calcd for C₂₄H₃₂O₄Na, 407.2193).

Poloncosidin F (**6**) colorless oil; $[\alpha]_D^{25} = +30$, c 0.10, MeOH; UV (MeOH) λ_{\max} (log ϵ) 232 (2.95) nm, 301 (2.68) nm; ECD (1.98 mM, MeOH) λ_{\max} ($\Delta\epsilon$) 210 (−3.36), 239 (−6.43), 300 (+3.40) nm; ¹H- and ¹³C-NMR data, Tables 1 and 2; HRESIMS m/z 405.2277 [M + H]⁺ (calcd for C₂₃H₃₃O₆, 405.2272).

3.4. Fermentation, Extraction and Isolation

Conformational searches were carried out using molecular mechanics with the MM+ method and HyperChem 8.0 software. Afterward, the geometries were optimized at the gas-phase B3LYP/6-31G(d) level in Gaussian09 software to identify the energy-minimized conformers. Then, the optimized conformers were subjected to the calculations of ECD spectra using the TD-DFT at the BH&HLYP/TZVP level. Simultaneously, the solvent effects of the MeOH solution were evaluated at the same DFT level using the SCRF/PCM method [18].

3.5. ECD Calculations

Conformational searches were carried out via molecular mechanics with the MM+ method in HyperChem 8.0 software. Afterward, the geometries were optimized at the gas-phase B3LYP/6-31G(d) level in Gaussian09 software to identify the energy-minimized conformers. Then, the optimized conformers were subjected to calculations of the ECD spectra using the TDDFT at the BH&HLYP/TZVP level. Simultaneously, solvent effects of the MeOH solution were evaluated at the same DFT level using the SCRFF/PCM method. [18]

3.6. Computational NMR Chemical Shift Calculations and DP4+ Analyses

All the theoretical calculations were performed using the Gaussian 09 program package. Conformational searches for possible isomers were conducted with molecular mechanics using the MMFF method with MacroModel software (Schrödinger, LLC) and the corresponding stable conformer, from which distributions higher than 2% were collected. Then, the B3LYP/6-31G(d) PCM level in DMSO was used to optimize the conformers. After that, the NMR shielding tensors of all optimized conformers were calculated using the DFT method at the mPW1PW91/6-31+G(d) PCM level on DMSO and then averaged based on Boltzmann's distribution theory [16]. GIAO (gauge-independent atomic orbital) NMR chemical calculations were performed using an equation described previously [19]. Finally, the NMR chemical shifts and shielding tensors (^1H and ^{13}C) were analyzed and compared with the experimental chemical shifts using DP4+ probability [16].

3.7. Antibacterial Assay

The antimicrobial activities of the isolated compounds against the human and aquatic pathogenic bacteria, *Aeromonas hydrophilia* QDIO-1, *Edwardsiella ictarda* QDIO-9, *E. tarda* QDIO-2, *Escherichia coli* EMBLC-1, *Klebsiella pneumoniae* EMBLC-3, *S. aureus* (MASA) EMBLC-4, *Micrococcus luteus* QDIO-3, *Pseudomonas aeruginosa* QDIO-4, *Vibrio alginolyticus* QDIO-5, *V. anguillarum* QDIO-6, *V. harveyi* QDIO-7, *V. parahemolyticus* QDIO-8, and *V. vulnificus* QDIO-10, and the plant pathogenic fungi *Alternaria solani* QDAU-1, *Colletotrichum gloeosporioides* QDAU-2, *Fusarium graminearum* QDAU-4, *F. oxysporum* QDAU-8, *Gaeumannomyces graminis* QDAU-21, *Rhizoctonia cerealis* QDAU-20, and *Valsa mali* QDAU-16 were determined with a serial dilution technique using 96-well microtiter plates as in our previous report [14]. The human and aquatic pathogenic bacteria and plant pathogenic fungi were supplied by the Institute of Oceanology, Chinese Academy of Sciences.

4. Conclusions

In summary, six new verrucosidin derivatives (1–6) were identified from the deep sea cold-seep-derived *Penicillium polonicum* CS-252. Compounds 1–5 represent the first examples of verrucosidins with a 2,5-dihydrofuran ring. The structures of these compounds were determined using a combination of methods (NMR, MS, ECD calculations and DP4+ probability analysis).

All these compounds were tested for antimicrobial activities. Compounds 4 and 6 displayed broad-spectrum inhibitory activity against *Escherichia coli* EMBLC-1, *Klebsiella pneumoniae* EMBLC-3, *Pseudomonas aeruginosa* QDIO-4, *Vibrio alginolyticus* QDIO-5, and *V. parahemolyticus* QDIO-8 with MIC values ranging from 4 to 32 $\mu\text{g}/\text{mL}$. Compound 1 showed activity against *P. aeruginosa* QDIO-4, *V. alginolyticus* QDIO-5, and *V. parahemolyticus* QDIO-8 with MIC values of 8.0, 8.0, and 4.0 $\mu\text{g}/\text{mL}$, respectively. Moreover, compound 7 was bactericidal against *P. aeruginosa* QDIO-4 and *V. parahemolyticus* QDIO-8 (each with an MIC value of 8.0 $\mu\text{g}/\text{mL}$).

Supplementary Materials: The following supporting information can be downloaded at: <https://www.mdpi.com/article/10.3390/ijms23105567/s1>. Selected 1D and 2D NMR and HRESIMS spectra of compounds 1–6; DP4+ probability analyses of compounds 4 and 5.

Author Contributions: Conceptualization, Y.L., H.L. and B.W.; Measurement, X.L. (Xiaoming Li); Data analysis, Y.L., X.L. (Xin Li) and S.Y.; Funding acquisition and project administration, B.W.;

Writing—original draft preparation, Y.L.; Writing—Review and editing, H.L. and B.W. All authors have read and agreed to the published version of the manuscript.

Funding: This work was financially supported by the Strategic Priority Research Program of the Chinese Academy of Sciences (XDA22050401), by the National Natural Science Foundation of China (U2006203 and 42076090), by the Senior User Project of RV KEXUE (KEXUE2020GZ02), and by the Shandong Provincial Natural Science Foundation (ZR2021ZD28).

Institutional Review Board Statement: Not applicable.

Informed Consent Statement: Not applicable.

Data Availability Statement: Not applicable.

Acknowledgments: B.-G.W. acknowledges the support of Oceanographic Data Center at IOCAS (for CPU time) and the RV KEXUE of the National Major Science and Technology Infrastructure from the Chinese Academy of Sciences (for sampling).

Conflicts of Interest: The authors declare no conflict of interest.

References

1. Li, W.; Ma, Z.H.; Chen, L.; Yin, W.B. Synthesis and production of the antitumor polyketide aurovertins and structurally related compounds. *Appl. Microbiol. Biotechnol.* **2018**, *102*, 6373–6381. [[CrossRef](#)] [[PubMed](#)]
2. Pan, C.Q.; Shi, Y.T.; Auckloo, B.N.; Chen, X.G.; Chen, C.T.A.; Tao, X.Y.; Wu, B. An unusual conformational isomer of verrucosidin backbone from a hydrothermal vent fungus, *Penicillium* sp. Y-50-10. *Mar. Drugs* **2016**, *14*, 156. [[CrossRef](#)] [[PubMed](#)]
3. Choo, S.J.; Park, H.R.; Ryoo, I.J.; Kim, J.P.; Yun, B.S.; Kim, C.J.; Shin-ya, K.; Yoo, I.D. Deoxyverrucosidin, a novel GRP78/BiP down-regulator, produced by *Penicillium* sp. *J. Antibiot.* **2005**, *58*, 210–213. [[CrossRef](#)] [[PubMed](#)]
4. Sonjak, S.; Frisvad, J.C.; Gunde-Cimerman, N. *Penicillium* mycobiota in arctic subglacial ice. *Microb. Ecol.* **2006**, *52*, 207–216. [[CrossRef](#)] [[PubMed](#)]
5. Guo, X.C.; Zhang, Y.H.; Gao, W.B.; Pan, L.; Zhu, H.J.; Cao, F. Absolute configurations and chitinase inhibitions of quinazoline-containing diketopiperazines from the marine-derived fungus *Penicillium polonicum*. *Mar. Drugs* **2020**, *14*, 156. [[CrossRef](#)] [[PubMed](#)]
6. Liu, S.Z.; Tang, X.X.; He, F.M.; Jia, J.X.; Hu, H.; Xie, B.Y.; Li, M.Y.; Qiu, Y.K. Two new compounds from a mangrove sediment-derived fungus *Penicillium polonicum* H175. *Nat. Prod. Res.* **2020**, *36*, 2370–2378. [[CrossRef](#)] [[PubMed](#)]
7. Ma, Y.R.; Wen, Y.Z.; Cheng, H.T.; Deng, J.T.; Peng, Y.; Bahetejiang, Y.; Huang, H.Q.; Wu, C.Q.; Yang, X.Z.; Pang, K.J. Penpolonin A–E, cytotoxic α -pyrone derivatives from *Penicillium polonicum*. *Bioorg. Med. Chem. Lett.* **2021**, *40*, 127921. [[CrossRef](#)] [[PubMed](#)]
8. Ding, G.Z.; Liu, J.; Wang, J.M.; Fang, L.; Yu, S.S. Secondary metabolites from the endophytic fungi *Penicillium polonicum* and *Aspergillus fumigatus*. *J. Asian. Nat. Prod. Res.* **2013**, *15*, 446–452. [[CrossRef](#)] [[PubMed](#)]
9. Elsunni, M.A.; Yang, Z.D. Secondary metabolites of the endophytic fungi *Penicillium polonicum* and their monoamine oxidase inhibitory activity. *Chem. Nat. Compd.* **2018**, *54*, 1018–1019. [[CrossRef](#)]
10. Abdel-Fatah, S.S.; El-Batal, A.I.; El-Sherbiny, G.M.; Khalafa, M.A.; El-Sayed, A.S. Production, bioprocess optimization and γ -irradiation of *Penicillium polonicum*, as a new Taxol producing endophyte from *Ginkgo biloba*. *Biotechnol. Rep.* **2021**, *30*, e00623. [[CrossRef](#)] [[PubMed](#)]
11. Valente, S.; Piombo, E.; Schroeckh, V.; Meloni, G.R.; Heinekamp, T.; Brakhage, A.A.; Spadaro, D. CRISPR-Cas9-based discovery of the verrucosidin biosynthesis gene cluster in *Penicillium polonicum*. *Front. Microbio.* **2021**, *12*, 660871. [[CrossRef](#)] [[PubMed](#)]
12. Aranda, E.; Rodríguez, M.; Benito, M.J.; Asensio, M.A.; Córdoba, J.J. Molecular cloning of verrucosidin-producing *Penicillium polonicum* genes by differential screening to obtain a DNA probe. *Int. J. Food Microbiol.* **2002**, *76*, 55–61. [[CrossRef](#)]
13. Meng, L.H.; Li, X.M.; Zhang, F.Z.; Wang, Y.N.; Wang, B.G. Talascortenes A–G, highly oxygenated diterpenoid acids from the sea-anemone-derived endozoic fungus *Talaromyces scorteus* AS-242. *J. Nat. Prod.* **2020**, *83*, 2528–2536. [[CrossRef](#)] [[PubMed](#)]
14. Cao, J.; Li, X.M.; Li, X.; Li, H.L.; Konuklugil, B.; Wang, B.G. Uncommon N-methoxyindole-diketopiperazines from *Acrostalagmus luteoalbus*, a marine algal isolate of endophytic fungus. *Chin. J. Chem.* **2021**, *39*, 2808–2814. [[CrossRef](#)]
15. Li, Y.H.; Li, X.M.; Li, X.; Yang, S.Q.; Shi, X.S.; Li, H.L.; Wang, B.G. Antibacterial alkaloids and polyketides from the deep sea-derived fungus *Penicillium cyclopium* SD-413. *Mar. Drugs* **2020**, *18*, 553. [[CrossRef](#)] [[PubMed](#)]
16. Grimblat, N.; Zanardi, M.M.; Sarotti, A.M. Beyond DP4: An improved probability for the stereochemical assignment of isomeric compounds using quantum chemical calculations of NMR shifts. *J. Org. Chem.* **2015**, *80*, 12526–12534. [[CrossRef](#)] [[PubMed](#)]
17. Zhang, H.P.; Timmermann, B.N. Withanolide structural revisions by ^{13}C NMR spectroscopic analysis inclusive of the γ -gauche effect. *J. Nat. Prod.* **2016**, *79*, 732–742. [[CrossRef](#)] [[PubMed](#)]
18. Frisch, M.J.; Trucks, G.W.; Schlegel, H.B.; Scuseria, G.E.; Robb, M.A.; Cheeseman, J.R.; Scalmani, G.; Barone, V.; Mennucci, B.; Petersson, G.A.; et al. *Gaussian09, Revision C.01*, Gaussian, Inc.: Wallingford, CT, USA, 2010.
19. Lee, S.R.; Lee, D.; Park, M.; Lee, J.C.; Park, H.; Kang, K.S.; Kim, C.; Beemelmans, C.; Kim, K.H. Absolute configuration and corrected NMR assignment of 17-hydroxycyclooctatin, a fused 5–8–5 tricyclic diterpene. *J. Nat. Prod.* **2020**, *83*, 354–361. [[CrossRef](#)] [[PubMed](#)]